JOURNAL OF CATALYSIS 10, 175–182 (1968)

Zeolitic Aluminosilicate

II. Surface Oxide Diffusion, Dynamic (Time Variant) Lewis Acids and Catalytic Activity with Hexane on Decationized Y

SHAO E TUNG AND EDWARD McININCH

From the Central Research Division Continental Oil Company, Ponca City, Oklahoma

Received October 19, 1967; revised December 5, 1967

Hexane cracking and isomerization on decationized Y catalysts were studied. The catalysts were found to deactivate. The catalysts with a higher percentage of decationization deactivate more readily, i.e., at a lower temperature. This deactivation is attributed to the surface reconstitution through the surface diffusion of oxide ions. The surface diffusion of the oxide ions imparts the *dynamic* (*time-variant*) characteristic to both the surface electric field and Lewis acids.

A concept of dynamic (time-variant) Lewis acids is proposed. The time variance characteristic renders these acid sites capable of both activated adsorption and subsequent desorption and, thereby, continuously promotes catalytic reactions in a cyclic manner.

INTRODUCTION

In the preceding paper (*1*) hexane cracking and isomerization with CaY catalyst were reported. Definite relationships between catalytic activities and surface electric field were observed. In this, we concurred with Pickert *et al.* (*2*) that these catalytic activities of CaY catalysts with respect to carbon–hydrogen bond activation are attributable to the electric field near surface ions. In addition, we further postulated that the surface field is *dynamic* (*time-variant*). This time variance of electrical field arises from the surface diffusion of the cations. This renders catalytic sites capable of both activated adsorption and subsequent desorption and thereby continuously promotes catalytic reactions in a cyclic manner.

The study is now extended to decationized Y catalysts. The results of this study are reported here.

EXPERIMENTAL PROCEDURE

The decationized zeolite (molecular sieve) was made by first exchanging the Na^+ with the NH_4^+ and subsequently decomposing the NH_4^+ by high-temperature calcination. The exchange was carried out on the same batch of NaY preparation using a 20% solution of NH_4Cl and dilutions thereof in exactly the same manner as for calcium exchange (*1*). The percent decationization, defined here as synonymous with the percent of the original Na^+ replaced, was determined to be 93% [noted henceforth as decationized (93%)Y], 85%, 75%, 61%, 47%, 36%, 25%, and 15%. The catalyst was first precalcined at 230°C and then calcined in situ in the microreactor at 550°C, as in the case of CaY catalyst. The same microreactor and reaction procedure were employed. Because of the comparatively higher activity of the decationized catalyst, the temperature levels studied were lowered. They ranged from 200° to 450° C at 50° increments. Both liquid products and gas products were collected and measured. Gas composition and liquid composition were secured by gas chromatographic and mass-spectrometric analyses in the same manner as was reported previously (*1*).

Some catalysts were found to deactivate during their use. Additional experiments were performed to learn about this deactivation.

Results

A. Rate and Product Distribution

The variation in rates is plotted versus the catalyst composition in Figs. 1 and 2. Figure 1 shows that the isomerization activity of the catalysts increases as temperature increases, reaches a maximum at 350°C, and then decreases on further increase in temperature. This activity decrease may be ascribed to the fact that isomerization and cracking are competitive reactions, and the high temperature favors cracking at the expense of the isomerization.

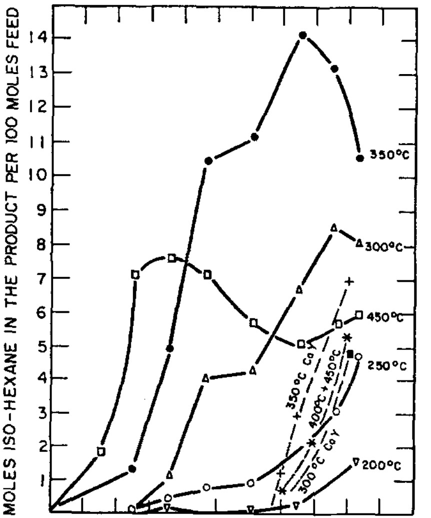

Fig. 1. Isomerization activity versus percent decationization of the catalysts.

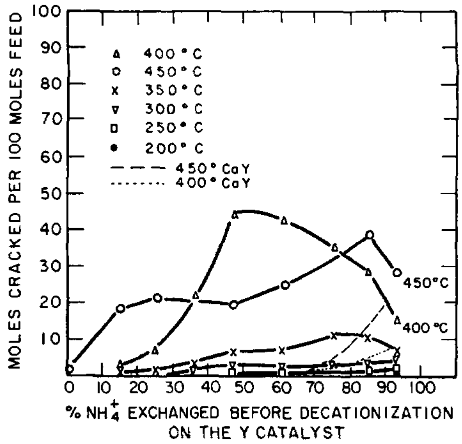

Fig. 2. Cracking activity versus percent decationization of the catalysts.

At a certain temperature level, the composition dependence also exhibits a maximum. For example, at 300°C, the peak isomerization activity was found to occur with decationized (85%)Y catalyst and decationized (93%)Y was less active. This suggests that the decationized (93%)Y could have been deactivated, for some reason, at this temperature level. It is to be noted that the peak positions shift toward the left side of the plot with the increase in the temperature level. From a deactivation point of view, it would mean that a catalyst with higher decationization level deactivates more readily or at a lower temperature. An approximate correlation between the catalyst composition (i.e., level of decantionization) and deactivation temperature is given in Fig. 3 where the solid line traces the peak composition of Fig. 1 and the dashed lines at both sides trace the compositions that represent the average between the peak composition of Fig. 1 and its two neighboring composition points. While the deactivations of the catalysts do not necessarily occur in exact coincidence with the peaks of Fig. 1, it must occur nearby these peak regions. Figure 3 suggests that a catalyst of a certain composition tends to deactivate when the temper-

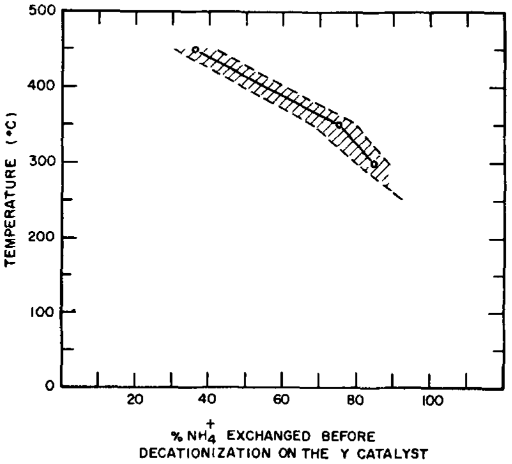

Fig. 3. Temperature of deactivation versus percent decationization of the catalysts.

ature reaches a point somewhere in the dashed line region. To the right of the dashed lines is the temperature region where the catalysts will deactivate.

This Fig. 3, derived from isomerization, activity, can be applied to the cracking activity as well. It explains the rather unusual activity reversal shown by the 400° and 450°C lines in Fig. 2. This activity reversal may be explained as follows: Below 36% decationization, the catalysts are not deactivated at 450°C; therefore, activity at 450°C is expectedly higher than that of the lower temperature; namely, 400°C. Between 36% and 75%, the catalysts are deactivated at 450°C, but they are not deactivated or deactivated as much at 400°C. An activity reversal is, therefore, observed. At 75% and above, catalysts are deactivated at both 450° and 400°C; and the activities of the catalysts at higher temperature thereby become higher again.

The dotted lines shown in Figs. 1 and 2 give the corresponding rates with the CaY catalysts (*1*). These lines indicate, in agreement with Rabo *et al.* (*3*), that the decationized catalysts are more active than the CaY catalysts of the comparable composition (i.e., same percent of Na^+ removal). In contrast to CaY catalysts, the activity of decationized catalysts was enhanced even at low percentages of decationization.

Some typical product distributions are summarized in Table 1. The saturates/unsaturates ratios for C_2 to C_5 aliphatics are quite high, especially at the lower temperatures. These ratios are higher than the corresponding ratios with the CaY catalysts (*1*).

B. Catalyst Deactivation

To confirm the observed catalyst deactivation, additional experiments were conducted where the variation of the cracking activity in terms of gas generation with the reaction duration at a certain temperature level was studied. A fresh batch of catalyst was used for the experiment conducted at each temperature level. Typical results for the decationized (47%)Y are presented in Fig. 4. In agreement with Figs. 2 and 3, the catalyst deactivates at 450°C; and the activity at that temperature level drops below that of 400°C. Similar plots were obtained for catalysts of other compositions. They all tend to confirm the deactivation curve of Fig. 3.

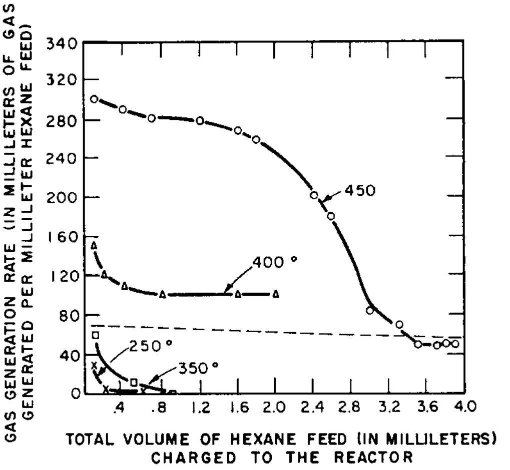

Fig. 4. Deactivation of decationized (47%) Y. (The dotted line shows the gas generation rate of the catalyst previously used at 450°C and recalcined in air at 550°C for 4 hr.)

Prolonged heating of the decationized (47%)Y catalyst at 450°C alone did not deactivate the catalyst. Therefore, deactivation occurred only after the hexane was admitted. Recalcination at 550°C in air of the deactivated catalyst failed to restore the catalytic activity. This is shown in Fig. 4. A deactivated catalyst at 450°C is shown to generate 52 ml of product gas per milliliter of hexane feed, while the same catalyst, after being recalcined in air at 550°C for 4 hr, generated about the same amount of gas product as is shown by the dotted line.

X-ray diffraction patterns for the decationized (47%)Y catalysts before and after the deactivation occurred were both taken, and no significant difference was detected.

DISCUSSION

A. Surface Sites

The decationization process has been discussed by Rabo *et al.*, (*4*) and Utterhoeven, Christner, and Hall (*5*). One scheme that

TABLE 1

PRODUCT DISTRIBUTION OF DECATIONIZED CATALYSTS—CONDENSED FORM

	Decationized Y (93%)					Decationized Y (75%)					Decationized Y (25%)				
	250°C	300°C	350°C	400°C	450°C	250°C	300°C	350°C	400°C	450°C	250°C	300°C	350°C	400°C	450°C
Reaction products (mole %)															
Hydrogen	—	—	0.03	2.08	12.15	—	—	.02	1.43	6.26	—	—	—	1.19	7.22
Hydrocarbons	100	100	99.97	97.92	87.85	100	100	99.98	98.57	93.74	100	100	100	98.81	92.78
Hydrocarbon distribution (on H_2- and C_6-free basis)															
Methane	—	—	0.04	5.91	15.76	—	—	0.24	4.05	11.02	—	—	—	4.22	23.05
Ethane	—	0.78	0.76	6.37	10.01	—	0.44	0.78	4.31	7.85	0.91	1.23	1.31	5.22	16.59
Ethylene															
Propane	11.98	17.72	26.44	38.61	36.71	19.50	20.17	32.63	47.01	45.07	23.64	23.31	33.74	39.54	34.97
Propylene	0.19	0.32	0.60	4.54	9.24	0.63	—	0.82	1.71	6.94	3.64	4.29	3.07	6.62	10.00
Isobutane	41.99	35.78	29.25	17.20	11.91	41.09	37.95	25.89	18.11	8.33	21.81	26.99	23.66	16.06	4.88
n-Butane	8.43	8.27	10.45	7.50	4.53	10.69	10.59	10.31	7.48	5.84	12.73	12.88	10.52	6.52	1.14
Isobutylene + Butene-1	—	—	—	0.31	1.91	—	—	0.02	0.05	0.50	—	—	2.19	1.00	0.36
trans-Butene-2	—	—	—	0.20	1.25	—	—	—	0.04	0.27	—	—	—	5.02	0.24
cis-Butene-2	—	—	—	0.15	0.92	—	—	—	0.03	0.21	—	—	—	3.01	0.18
Isopentanes	28.57	24.07	23.08	11.94	2.84	21.17	23.66	21.11	10.71	4.52	18.18	19.63	15.78	12.84	3.80
n-Pentanes	6.16	5.23	5.05	2.29	0.76	6.91	5.14	4.71	2.45	1.73	8.18	4.29	4.82	3.01	1.37
Pentenes	—	—	—	0.15	0.15	—	—	—	—	0.22	10.91	7.36	6.13	5.02	0.15
Benzene	—	—	—	0.41	0.22	—	—	—	0.27	0.83	—	—	—	—	0.36
Xylene	2.68	1.95	1.08	1.61	0.87	—	2.10	0.58	0.80	2.16	—	—	4.29	0.93	0.72
Toluene	—	3.90	2.17	2.02	1.97	—	—	1.75	1.23	3.19	—	—	—	1.80	1.82
C_3-Substituted Benzene	—	1.95	1.08	0.81	0.55	—	—	1.17	0.41	0.83	—	—	—	0.90	0.36
Naphthalene	—	—	—	—	0.11	—	—	—	—	0.16	—	—	—	—	—
2-Methylnaphthalene	—	—	—	—	0.11	—	—	—	—	0.16	—	—	—	—	—
1,2-Dimethylnaphthalene	—	—	—	—	0.11	—	—	—	—	0.16	—	—	—	—	—
Aliphatic C_6 distribution															
n-Hexane	95.16	91.61	88.59	88.33	91.14	98.40	93.30	84.00	80.50	93.00	99.87	99.82	98.65	96.00	95.10
2-Methylpentane	2.48	4.29	5.65	6.01	4.32	0.78	3.54	7.96	9.82	3.61	0.06	0.10	0.71	3.04	2.48
3-Methylpentane	1.49	2.73	3.98	4.06	3.27	0.45	2.16	5.42	7.12	2.52	0.04	0.05	0.38	1.36	1.69
2,2-Dimethylpentane	0.19	0.30	0.38	0.25	0.22	0.05	0.21	0.46	0.44	0.14	0.01	0.01	0.03	0.10	0.09
2,3-Dimethylpentane	0.68	1.06	1.40	1.35	1.05	0.24	0.94	2.12	2.30	0.69	0.02	0.03	0.24	0.56	0.54

is in accord with infrared evidence has been suggested as follows:*

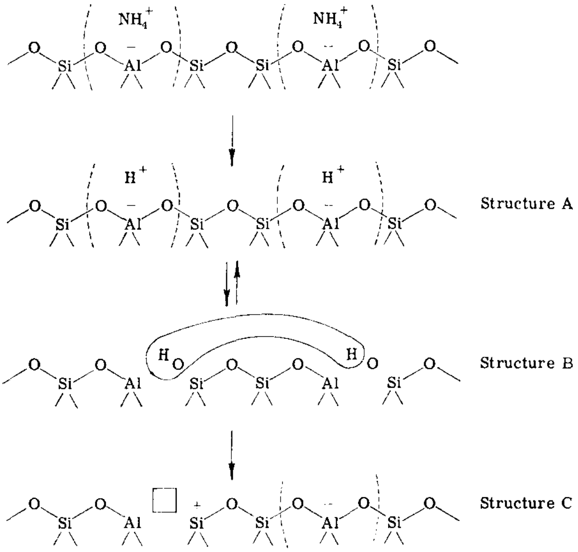

Upon deamination, classical Brönsted acids (Structure A) are generated. At room temperature, IR evidence indicated that the equilibrium is in favor of the hydroxyl formation (Structure B); nevertheless, protons are readily available upon the approach of a base or at high temperature levels.

The three-coordinated aluminum ions (Structure B), when accessible to foreign molecules, may function as conventional Lewis acids (*5*). Upon dehydroxylation, a surface group, consisting of an accessible three-coordinated aluminum ion, adjacent to a three-coordinated silicon ion, is formed. Both the aluminum and the silicon ions may function as Lewis acids. In addition, a surface field is created between the positively charged silicon ion and negatively charged $(AlO_2)^-$ group.

The surface protons are undoubtedly important for a host of chemical reactions (e.g., alkylation, dealkylation, and olefin polymerization). For carbon–hydrogen bond activation, however, on account of the fact that silica-alumina surfaces are virtually ineffective, we believe (*1*) that the reaction sites most probably rest upon either the Lewis acids or the surface electric fields.

B. Surface Diffusion and Catalyst Deactivation

Deactivation of catalysts may arise from (1) carbon deposition; (2) collapse of the crystal structure; (3) surface reconstitution.

The carbon deposition deactivation is unlikely because recalcination of the deactivated catalyst in air did not restore its activity (Fig. 4). Collapse of crystal structure was not indicated by the X-ray diffraction pattern. The deactivation is most probably due to surface reconstitution.

While one representation of the decationized process was discussed, the actual process is most likely more complex and may generate a number of different kinds of surface groups or coexisting surface sites. The distributions of these surface groups, as first formed are not in their lowest energy states. Relaxation toward the lower energy states, however, may be a slow process at room temperature. One way to achieve this surface relaxation or reconstitution is through diffusion. The decationized Y catalysts, after deamination and dehydroxylation, probably have one oxygen vacancy for every two original ammonium cations in fully dehydroxylated form. No activation energy for generating vacancies

---

* The square denotes an oxygen vacancy.

for diffusional purposes is needed. The overall diffusional energy for the oxide ions could be fairly low. Deactivation, as observed, may be attributed to the relaxation of the surface from one distribution of the surface sites to another. The latter distribution has the lower energy and is correspondingly less active. An alternative and more specific relationship between surface diffusion and deactivation will be discussed in the next section after some discussion of the reaction mechanism.

When the diffusion is promoted thermally, we have thermal relaxation. In our present case, prolonged heating at 450°C alone did not deactivate the decationized (47%)Y catalyst. This indicates that the thermal energy at 450°C was not quite sufficient to overcome the energy barrier for diffusion of this particular catalyst. Additional promotion by the interaction of the *n*-hexane with the catalyst surface was necessary to deactivate the catalyst.

The fact that the deactivation was promoted by the hexane–surface interaction tends to corroborate the view that diffusion plays a significant role in deactivation. Interaction of hexane with the surface field tends to diminish surface field potential and hence the diffusional energy barrier (*1*, *6*). With the NaX catalyst, Stamires (*6*) reported a decrease in activation energy or an increase in electrical conductivity upon the adsorption of *n*-hexane. Although only remotely related, we may also cite the discussion of the surface reconstitution of the nickel 110 face upon adsorption of foreign atoms by Germer and MacRae (*7*).

In evaluating catalytic activity of the decationized Y catalysts, the catalyst deactivation should be considered.

C. Surface Diffusion and Catalytic Activity

The diffusion of surface oxide ions has significant bearing upon the catalytic activity of the decationized Y catalysts. In the preceding paper (1), it was suggested that diffusion of cations (e.g., Ca^{2+}) in CaY catalyst makes the surface electric field on that catalyst *dynamic* (*time-variant*). The importance of time variance of the field in the overall reaction was pointed out. Similarly, oxide diffusion will also render the surface field dynamic (time-variant) with the same effect on its catalytic activity. This may be illustrated as follows:

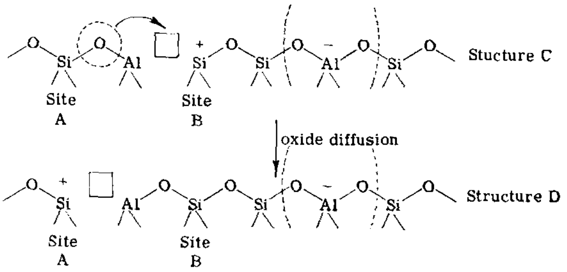

From Structure C to Structure D, the positively charged silicon ion becomes more remote from the negatively charged $(AlO)_2^-$ group. The field strength correspondingly decreases. That the fluctuation of the surface field renders catalyst sites capable of both activated adsorption and desorption and thereby continuously promotes catalytic reactions in a cyclic manner has been discussed in detail in the preceding paper and need not be repeated here.

We would like to point out in this communication that the strength of Lewis acids also varies in accordance with the movement of oxide ions on the surfaces. Referring to the previous representations, we may observe that, with Structure C (before the oxide diffusion), site A is neutral and site B is a Lewis acid; but, with Structure D (after the oxide diffusion), site A becomes a Lewis acid and site B is neutral. Because of this dynamic (time-variant) characteristic, a Lewis acid site (denoted by L^+), which may otherwise be ineffective in inducing the following cyclic reactions,

$$L^+ + C_6 \rightarrow L^+H^- + C_6^+ \quad (1)$$

$$C_6^+ \rightarrow C_6^+ \text{ (iso)} \quad (2)$$

$$L^+H^- + C_6^+ \text{ (iso)} \rightarrow L^+ + C_6 \text{ (iso)} \quad (3)$$

$$\overline{L^+ + C_6 \rightarrow L^+ + C_6 \text{ (iso)}}$$

because the hydride L^+H^- in reaction (3) is too strongly bonded to the Lewis acid site, may now induce the reaction cycle smoothly as follows:*

$$L_1^+ + C_6 \rightarrow L_1^+H^- + C_6^+ \qquad (4)$$

$$C_6^+ \rightarrow C_6^+ \text{ (iso)} \qquad (5)$$

$$L_1^+H^- \xrightarrow{\text{Oxide diffusion}} L_1H^- \qquad (6)$$

$$L_1H^- + C_6^+ \text{ (iso)} \rightarrow L_1 + C_6 \text{ (iso)} \qquad (7)$$

$$L_2 \xrightarrow{\text{Oxide diffusion}} L_2^+ \qquad (8)$$

$$L_1^+ + C_6 + L_2 \rightarrow L_1 + C_6 \text{ (iso)} + L_2^+ \qquad (9)$$

Similarly, cracking may proceed in the following manner:

$$L_1^+ + C_6 \rightarrow L_1^+H^- + C_6^+ \qquad (10)$$

$$C_6^+ \rightarrow C_n^+ + C_{6-n} \text{ (olefin)} \qquad (11)$$

$$L_1^+H^- \xrightarrow{\text{Oxide diffusion}} L_1H^- \qquad (12)$$

$$L_1H^- + C_n^+ \rightarrow L_1 + C_n \qquad (13)$$

$$L_2 \xrightarrow{\text{Oxide diffusion}} L_2^+ \qquad (14)$$

$$L_1^+ + C_6 + L_2 \rightarrow L_1 + C_n + C_{6-n} \text{ (olefin)} + L_2^+ \qquad (15)$$

It is to be pointed out that Eqs. (1) to (15) are merely the formal representations of the actual reactions occurred. We are not proposing that full ionization of carbon–hydrogen bonds is necessary. It is possible that the carbon–hydrogen bonds only need to be sufficiently polarized that they impart into their polarization terminals enough ionic properties that the isomerization or cracking steps (5) and (11) may occur.

Hydride ion, on account of its small size, does not block oxide diffusion. Thus, we may visualize the diffusion as follows:

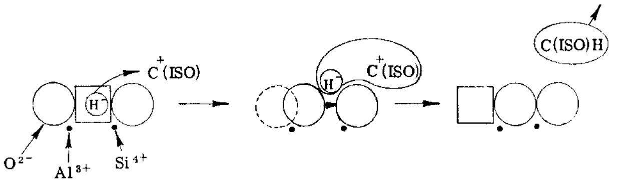

It may be seen that the dislodging of the hydride ion is related to the proximity of the carbonium ion with which it combines. Since the carbonium ions tend to situate themselves nearby the negatively charged $(AlO_2)^-$ groups, the close proximity of these groups to the Lewis acid sites is beneficial to the hydride dislodging and perhaps the overall reaction rate if the former is the rate-controlling step. From this viewpoint, the deactivation of a catalyst could be a direct consequence of the oxide diffusion which might result in a larger separation between a Lewis acid site and an $(AlO_2)^-$ group (e.g., Structure C changes to Structure D).

Because of this dynamic (time-variant) characteristics, the Lewis acids on decationized Y could behave in a radically different way from the Lewis acids on other catalyst surfaces, e.g., silica-alumina, on the surface of which the oxide ions may not diffuse as readily. It is conceivable that the Lewis acids could promote carbon–hydrogen bond activation on decationized Y catalyst and not on the silica-alumina surfaces.

On the CaY catalysts, the carbon–hydrogen bond activation is essentially by the surface field. Few Lewis acids exist. On the decationized Y catalyst, both Lewis acids and surface fields can be effective. This is reflected by the high activity of the decationized Y catalysts. Furthermore, while the surface field on a CaY catalyst does not come into being below 50–60% Na^+ removal, the Lewis acids and the field are created even at low percentage of decationization. This is also reflected by the experimental data.

REFERENCES

1. Tung, Shao E, and McIninch, E., *J. Catalysis* **10,** 166 (1968).
2. Pickert, P. E., Rabo, J. A., Dempsey, E., and Shomaker, V., *Proc. Intern. Congr. Catalysis,*

---

[*] C_6, C_6(iso), C_6^+, C_{6-n}(olefin) denote C_6H_{14}, iso-C_6H_{14}, $C_6H_3^+$, $C_{6-n}H_{12-2n}$ with $n < 6$, etc.

3rd, Amsterdam, 1964, **1,** 714 (North-Holland Publ. Co., Amsterdam, 1965).

3. RABO, J. A., PLAINS, W., PICKERT, P. E., AND BOYLE, J. E., U. S. Patent 3,236,761 and U. S. Patent 3,236,762.
4. RABO, J. A., PICKERT, P. E., STAMIRES, D. N., AND BOYLE, J. E., *Actes Congr. Intern. Catalyse, 2ᵉ Paris, 1961,* p. 2055 Editions Technip, Paris, (1961).
5. UTTERHOEVEN, J. B., CHRISTNER, L. G., AND HALL, W. K., *J. Phys. Chem.* **69,** 2117 (1965).
6. STAMIRES, D. N., *J. Chem. Phys.* **36,** 3174 (1962).
7. GERMER, L. H., AND MACRAE, A. U., *Proc. Natl. Acad. Sci. (U. S.)* **48,** 999 (1962).